

High-Accuracy Polishing Technique Using Dwell Time Adjustment

S. Satake^{1,*}, K. Yamamoto¹ and S. Igarashi¹

¹ *Department of Applied Electronics, Tokyo University of Science, 2641 Yamazaki, Noda, Chiba 278-8510, Japan.*

Received 30 August 2005; Accepted (in revised version) 11 November 2005

Communicated by Takashi Yabe

Abstract. Two algorithms for dwell time adjustment are evaluated under the same polishing conditions that involve tool and work distributions. Both methods are based on Preston's hypothesis. The first method is a convolution algorithm based on the Fast Fourier Transform. The second is an iterative method based on a constraint problem, extended from a one-dimensional formulation to address a two-dimensional problem. Both methods are investigated for their computational cost, accuracy, and polishing shapes. The convolution method has high accuracy and high speed. The constraint problem on the other hand is slow even when it requires larger memory and thus is more costly. However, unlike the other case a negative region in the polishing shape is not predicted here. Furthermore, new techniques are devised by combining the two methods.

Key words: Polishing; surface grinding; dwell time; convolution method; fast Fourier transform; constraint problem.

1 Introduction

Recently, the focus on the processing of high-precision optical elements into target shapes has shifted to surface creation technology using polishing heads that can control the amount of material removed [1–6]. This technology is known as corrective polishing method where polishing shape is given by scanning the variable velocity of the polishing head on the work surface of a physical object and by controlling the dwell time of the polishing head. It is known that the accuracy demanded for modern optical elements is extended to the order of nanometer. Moreover, the polishing areas are becoming larger

*Correspondence to: S. Satake, Department of Applied Electronics, Tokyo University of Science, 2641 Yamazaki, Noda, Chiba 278-8510, Japan. Email: satake@te.noda.tus.ac.jp

and posing new challenges for the polishing techniques especially when it takes longer time to complete the task. Also, the calculating algorithm for the dwell time distribution to determine processing accuracy and cost are becoming increasingly more important.

In one calculation method, the amount of material removed is estimated using a model equation that accounts for the polishing velocity, the switching processes and anti-processes at each point, and the technique for finishing the target shape [7]. However, in this method the amount of material removed in one scan is considered to be uniform but the dwell time distribution cannot be obtained. Hence, a method for calculating the dwell time distribution with a fast Fourier transform (FFT) was proposed by Negishi et al. [8] which is one of the two methods addressed in this paper. The other method evolved from a technique for solving one dimensional algorithm for the dwell time calculation as a constraint problem and was developed by Yang et al. [9].

In this current study, the technique for obtaining the dwell time distribution by the one-dimensional algorithm for constraint problem is extended to address a two-dimensional problem which is more appropriate for actual surfaces. This technique is then compared with the FFT calculation technique, and the characteristics of the two techniques are analyzed later in this paper. Furthermore, new techniques are designed by combining the two methods.

2 Two techniques for solving the dwell time distribution

Polishing removal is based on a convolution model [3] derived from Preston's hypothesis. The unit removal shape is obtained from a polishing experiment with a polishing head driven for a unit time. The model is expressed by an integration of a convolution equation over the grinding area A :

$$h(x, y) = \int_{\mathbf{A}} g(u, v) f(u - x, v - y) dudv, \quad (2.1)$$

where $h(x, y)$ is removal shape, $g(u, v)$ is dwell time distribution, $f(x, y)$ is unit removal shape, and x, y, u, v are variables. Moreover, polishing adjustment progresses by bringing the removal shape close to the error shape, which is defined as the difference between the work shape and the architectonic shape:

$$d(x, y) = h(x, y) + e(x, y), \quad (2.2)$$

where $d(x, y)$ is the error shape, i.e., the target removal shape measured by a shape measurement device and $e(x, y)$ is the residual error shape that cannot be modified. It is necessary to calculate the dwell time distribution g from the target removal shape d and unit removal shape f during polishing adjustment. The concept of convolution is shown in Fig. 2.

We first describe the technique for calculating $d(x, y)$ the dwell time distribution by FFT [9]. During the calculation, the following conditions are to be met for polishing adjustment:

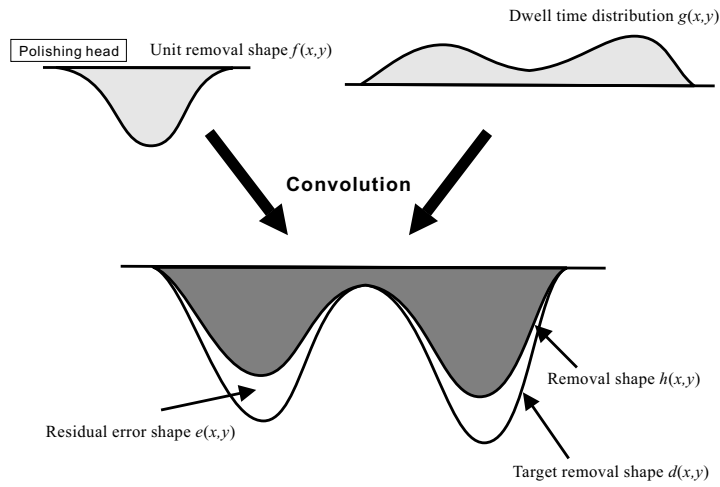


Figure 1: Convolution model.

1. The dwell time remain positive over the entire region.
2. The residual error be reduced.
3. The processing time be reduced.
4. The width of the change in the dwell time distribution be reduced.

By applying the Fourier transform the Eq. (2.2) turns into the equation

$$D(\omega_x, \omega_y) = G(\omega_x, \omega_y)F(\omega_x, \omega_y) + E(\omega_x, \omega_y), \tag{2.3}$$

where $D(\omega_x, \omega_y)$ is the Fourier transform of $d(x, y)$, abbreviated as D . An instinctive method, which consists of defining $E = 0$, calculating $G = D/F$, performing the inverse Fourier transform, and obtaining the dwell time G is not reliable: the method is divergent when $|F|$ is small. Hence, the filter function $Q(\omega_x, \omega_y)$ is used to calculate the dwell time:

$$G = QD/F. \tag{2.4}$$

Consequently, we use

$$E = (1 - Q)D \tag{2.5}$$

and express Q as

$$Q(\omega_x, \omega_y) = a(\omega_x, \omega_y) + b(\omega_x, \omega_y)j, \tag{2.6}$$

with real functions $a(\omega_x, \omega_y)$ and $b(\omega_x, \omega_y)$. Here, j is the imaginary unit. The forms of $a(\omega_x, \omega_y)$ and $b(\omega_x, \omega_y)$ are obtained by minimizing the following functional:

$$S = \int_A |e(x, y)|^2 dx dy + \alpha \int_A |g(x, y)|^2 dx dy. \tag{2.7}$$

The first term on the right-hand side of (2.7) is the residual error, the second term is the dwell time distribution to the second power, and α is a weighting factor to suppress residual error when it is small and to suppress a large stay time. The following equations are obtained from Parseval's formula:

$$\begin{aligned} \int_A |e(x, y)|^2 dx dy &= \int_W |E(\omega_x, \omega_y)|^2 d\omega_x d\omega_y \\ \int_A |g(x, y)|^2 dx dy &= \int_W |G(\omega_x, \omega_y)|^2 d\omega_x d\omega_y. \end{aligned} \quad (2.8)$$

We can use the upper expressions to rewrite Eq. (2.7):

$$S = \int_W \left\{ ((a-1)^2 + b^2) |F|^2 + \alpha(a^2 + b^2) \right\} |D/F|^2 d\omega_x d\omega_y. \quad (2.9)$$

This can be expressed as an integral of the function $s(a(\omega_x, \omega_y), b(\omega_x, \omega_y), \omega_x, \omega_y)$. By making the functional S undescended by the variation principle, i.e.,

$$\frac{\partial s}{\partial a} = \frac{\partial s}{\partial b} = 0, \quad (2.10)$$

the following results are obtained:

$$a(\omega_x, \omega_y) = \frac{|F(\omega_x, \omega_y)|^2}{\alpha + |F(\omega_x, \omega_y)|^2}, \quad b(\omega_x, \omega_y) = 0. \quad (2.11)$$

In practice, since the weighting factor must not depend on the unit removal shape and must be constant, α is transformed into the dimensionless weighting factor $\beta = \alpha / |F(0, 0)|^2$. Consequently,

$$Q(\omega_x, \omega_y) = \frac{|F(\omega_x, \omega_y)|^2}{\beta |F(0, 0)|^2 + |F(\omega_x, \omega_y)|^2}. \quad (2.12)$$

It may be considered that the calculated residual error is the target removal shape in the method described above again, and improvement may be made by using some iterative techniques. Note that in this method, a negative value for the dwell time may be obtained as the method does not take care of the sign of the dwell time. In this case, the negative value is replaced by zero.

We next describe the technique for solving the dwell time distribution as a constraint problem. First we describe the one-dimensional problem [9] and then consider the two-dimensional case. The following conditions must be satisfied for polishing adjustments:

1. The dwell time be not negative at any point over the entire region;
2. The residual error be not negative at any point over the four corners;
3. The variation of the interior, connectivity, and copy shape of the dwell time distribution remain smooth.

This constraint problem can be modeled using vectors and matrices. In one dimension, for n data points, let X be an n -dimensional vector representing the dwell time, A an $n \times n$ matrix, and B an n -dimensional vector representing the residual error shape:

$$X = \begin{pmatrix} x_1 \\ x_2 \\ \vdots \\ x_n \end{pmatrix}, \quad A = \begin{pmatrix} a_{11} & a_{12} & \cdots & a_{1n} \\ a_{21} & a_{22} & \cdots & a_{2n} \\ \vdots & \vdots & & \vdots \\ a_{n1} & a_{n2} & \cdots & a_{nn} \end{pmatrix}, \quad B = \begin{pmatrix} b_1 \\ b_2 \\ \vdots \\ b_n \end{pmatrix}. \quad (2.13)$$

Then, the problem can be formulated as:

$$\begin{aligned} \text{Constraint equation:} & \quad AX \leq B \\ \text{Nonnegative condition:} & \quad X \geq 0 \\ \text{Goal:} & \quad B - AX \rightarrow \text{minimum,} \end{aligned}$$

where the matrix A is determined by the unit removal shape of the polishing head. The one-dimensional unit removal shape data Z is assumed to be a row vector,

$$Z = (c_{-m} \quad c_{-m+1} \quad \cdots \quad c_0 \quad \cdots \quad c_k), \quad m + k + 1 \ll n, \quad (2.14)$$

where c_0 is the unit removal in the center of the polishing head. The number of unit removal data elements is $m + k + 1$. Then

$$A = \begin{pmatrix} c_0 & c_0 & \cdots & c_k & 0 & \cdots & 0 & \cdots & 0 \\ c_0 & c_0 & \cdots & c_{k-1} & c_k & \cdots & 0 & \cdots & 0 \\ \vdots & \vdots & & \vdots & \vdots & & \vdots & & \vdots \\ 0 & 0 & \cdots & 0 & 0 & \cdots & c_{-m} & \cdots & c_0 \end{pmatrix}. \quad (2.15)$$

Developing the modeling constraint equation gives

$$\sum_{i=1}^n a_{ji} x_i = b_j, \quad j = 1, \dots, n. \quad (2.16)$$

The maximum possible dwell time x_i $i = 1, \dots, n$, is limited by the amount of error b_j at each point:

$$x_i \leq \frac{1}{N} \min \{b_j / a_{ji} : j = 1, \dots, n; a_{ji} \neq 0.\} \quad (2.17)$$

The amount of polishing at a certain point is found by overlapping the polishing that contributes to that point. To ensure that the dwell time distribution is smooth, the dwell time that contributes to a certain point is allocated proportionally and evenly:

$$x_i = \frac{1}{N} \min \{b_j / a_{ji} : j = 1, \dots, n; a_{ji} \neq 0.\} \quad (2.18)$$

As the number of unit removal shape data elements is $m + k + 1$, N is assumed to satisfy

$$N \geq m + k + 1. \quad (2.19)$$

In addition, the remaining residual error E is calculated as follows:

$$E = B - AX. \quad (2.20)$$

The residual error can not be minimized by only one cycle of the calculation using an even allocation of the dwell time. However, the residual error can be reduced by repeating the calculation until it converges to a certain nonnegative constant. This constant is the residual error that cannot be corrected and remains unchanged. In short, X_p is the dwell time obtained by repeating the calculation p times with B_p the error shape:

$$X_p = \begin{pmatrix} x_1^{(p)} \\ x_2^{(p)} \\ \vdots \\ x_n^{(p)} \end{pmatrix}, \quad B_p = \begin{pmatrix} b_1^{(p)} \\ b_2^{(p)} \\ \vdots \\ b_n^{(p)} \end{pmatrix}. \quad (2.21)$$

The final dwell time X is given by

$$X = \sum_p X_p. \quad (2.22)$$

Moreover, we have

$$x_i = \frac{1}{N} \min \{b_j/a_{ji} : j = 1, \dots, n; a_{ji} \neq 0\}, \quad (2.23)$$

and the minimized residual error E is given by

$$E = B - \sum_p AX_p. \quad (2.24)$$

For two-dimensional modeling, the number of data points is $m \times n$, X is an $m \times n$ matrix representing the dwell time, A is a four-dimensional $m \times n \times m \times n$ matrix, and B is an $m \times n$ matrix representing the error shape:

$$X = \begin{pmatrix} x_{11} & x_{12} & \cdots & x_{1n} \\ x_{21} & x_{22} & \cdots & x_{2n} \\ \vdots & \vdots & & \vdots \\ x_{m1} & x_{m2} & \cdots & x_{mn} \end{pmatrix}, \quad B = \begin{pmatrix} b_{11} & b_{12} & \cdots & b_{1n} \\ b_{21} & b_{22} & \cdots & b_{2n} \\ \vdots & \vdots & & \vdots \\ b_{m1} & b_{m2} & \cdots & b_{mn} \end{pmatrix}. \quad (2.25)$$

The factor of A is defined as a_{ijkl} , $1 \leq i, k \leq m$, $1 \leq j, l \leq n$. The two-dimensional problem then becomes

$$\begin{aligned} \text{Constraint equation:} & \quad AX \leq B \\ \text{Nonnegative condition:} & \quad X \geq 0 \\ \text{Goal:} & \quad B - AX \rightarrow \text{minimum,} \end{aligned}$$

where AX is an operation for a matrix A determined by the unit removal shape of the polishing head:

$$AX = \sum_{i=1}^m \sum_{j=1}^n a_{ijkl} x_{ij}, \quad k = 1, \dots, m, \quad l = 1, \dots, n. \tag{2.26}$$

Assume the two-dimensional unit removal shape data to be represented by the matrix

$$Z = \begin{pmatrix} c_{-q-s} & \cdots & c_{-q0} & \cdots & c_{-qp} \\ \vdots & & \vdots & & \vdots \\ c_{0-s} & \cdots & c_{00} & \cdots & c_{0p} \\ \vdots & & \vdots & & \vdots \\ c_{r-s} & \cdots & c_{r0} & \cdots & c_{rp} \end{pmatrix}, \quad s + p + 1 \ll m, \quad q + r + 1 \ll n, \tag{2.27}$$

where c_{00} is the unit removal shape at the center of the polishing head. The number of two-dimensional unit removal shape data elements is $(s + p + 1) \times (q + r + 1)$. This gives

$$a_{ij11} = \begin{pmatrix} c_{00} & c_{01} & \cdots & c_{0r} & 0 & \cdots & 0 \\ c_{10} & c_{11} & \cdots & c_{1r} & 0 & \cdots & 0 \\ \vdots & \vdots & & \vdots & \vdots & & \vdots \\ c_{p0} & c_{p1} & \cdots & c_{pr} & 0 & \cdots & 0 \\ 0 & 0 & \cdots & 0 & 0 & \cdots & 0 \\ \vdots & \vdots & & \vdots & \vdots & & \vdots \\ 0 & 0 & \cdots & 0 & 0 & \cdots & 0 \end{pmatrix}. \tag{2.28}$$

It follows from the modeling constraint equation that

$$\sum_{i=1}^m \sum_{j=1}^n a_{ijkl} x_{ij} = b_{kl}, \quad k = 1, \dots, m, \quad l = 1, \dots, n. \tag{2.29}$$

The maximum possible dwell time x_{ij} , $1 \leq i \leq m$, $1 \leq j \leq n$, is limited to the amount of error b_{kl} at each point, i.e.,

$$x_{ij} \leq \min \{ b_{kl} / a_{ijkl} : k = 1, \dots, m; l = 1, \dots, n; a_{ijkl} \neq 0 \}. \tag{2.30}$$

The amount of polishing becomes

$$x_{ij} = \frac{1}{MN} \min \{b_{kl}/a_{ijkl} : k = 1, \dots, m; l = 1, \dots, n; a_{ijkl} \neq 0\}. \quad (2.31)$$

As the number of unit removal shape data elements is $(s + p + 1) \times (q + r + 1)$, M and N are assumed to be

$$M \geq m + k + 1, \quad N \geq m + k + 1. \quad (2.32)$$

The remaining residual error E is then given by

$$E = B - AX. \quad (2.33)$$

The residual error is reduced by repeating calculations until a nonnegative constant is obtained. X_p is the dwell time obtained by p calculations, with B_p the error shape:

$$X_p = \begin{pmatrix} x_{11}^{(p)} & x_{12}^{(p)} & \cdots & x_{1n}^{(p)} \\ x_{21}^{(p)} & x_{22}^{(p)} & \cdots & x_{2n}^{(p)} \\ \vdots & \vdots & & \vdots \\ x_{m1}^{(p)} & x_{m2}^{(p)} & \cdots & x_{mn}^{(p)} \end{pmatrix}, \quad B_p = \begin{pmatrix} b_{11}^{(p)} & b_{12}^{(p)} & \cdots & b_{1n}^{(p)} \\ b_{21}^{(p)} & b_{22}^{(p)} & \cdots & b_{2n}^{(p)} \\ \vdots & \vdots & & \vdots \\ b_{m1}^{(p)} & b_{m2}^{(p)} & \cdots & b_{mn}^{(p)} \end{pmatrix}. \quad (2.34)$$

Again the final dwell time X is given by $X = \sum_p X_p$, and the minimized residual error E is $E = B - \sum_p AX_p$.

3 Combined algorithm

The two techniques mentioned above can be combined in two different ways. We consider and compare the ways of combining the two techniques. The two possible combined algorithms are:

- (1) calculating the removal shape by the FFT calculation technique (Method A) and calculating the target removal shape by the constraint problem calculation technique (Method B) known as the A-B Method; and
- (2) calculating the removal shape by Method B and calculating the target removal shape by Method A known as B-A Method.

The number of iterations is set from the value when for each method the peak value (PV) and root mean square (RMS) of the residual error converge. The flow charts of the two calculation methods and the two combined algorithms are shown in Figs. 2-5.

4 Computational results

In this section, the dwell time algorithm is calculated by the two methods (A and B), and the characteristics of both methods are then evaluated. For the calculation the column-shaped target removal shape and the Gaussian unit removal shape per minute are shown

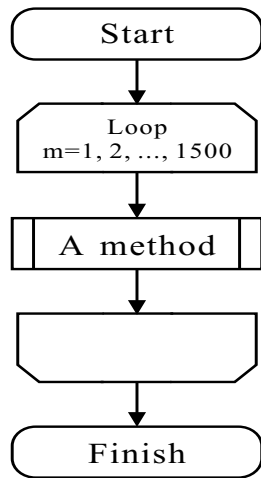


Figure 2: Flow chart of Method A.

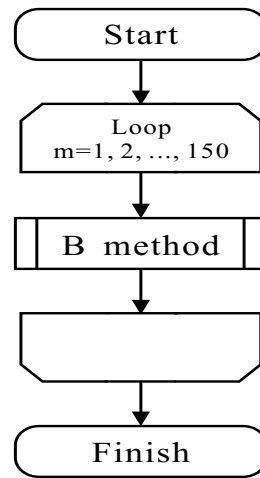


Figure 3: Flow chart of Method B.

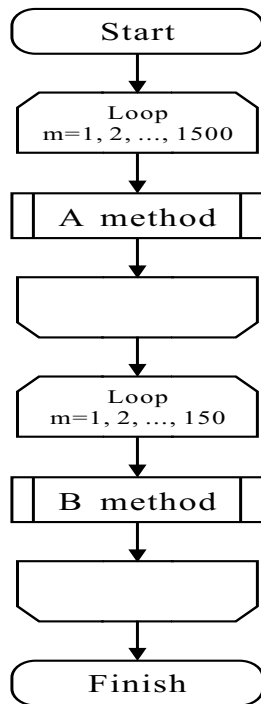


Figure 4: Flow chart of A-B Method.

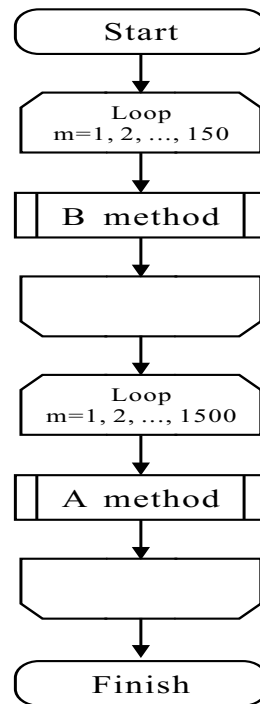


Figure 5: Flow chart of B-A Method.

in Fig. 6; and the cross-section views are shown in Fig. 7. The number of data point in the calculation is 64×64 .

The results for the removal shape produced by the Methods A and B obtained from the

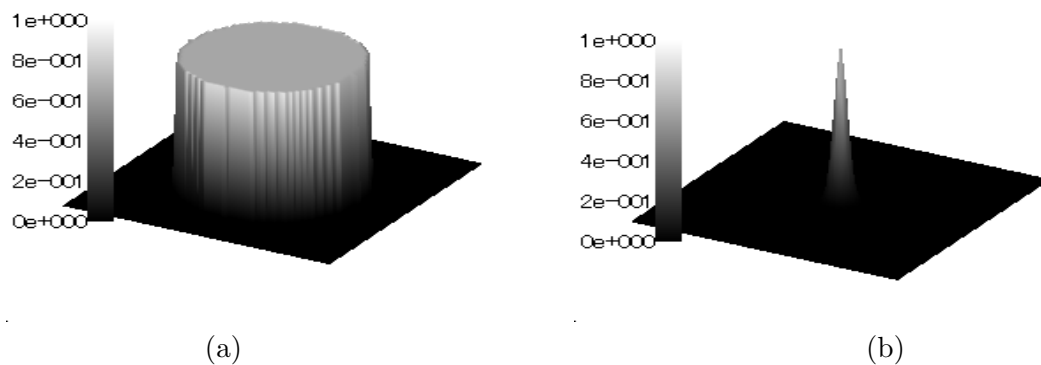


Figure 6: (a): Two-dimensional column-shaped target removal shape; and (b): Two-dimensional Gaussian unit removal shape.

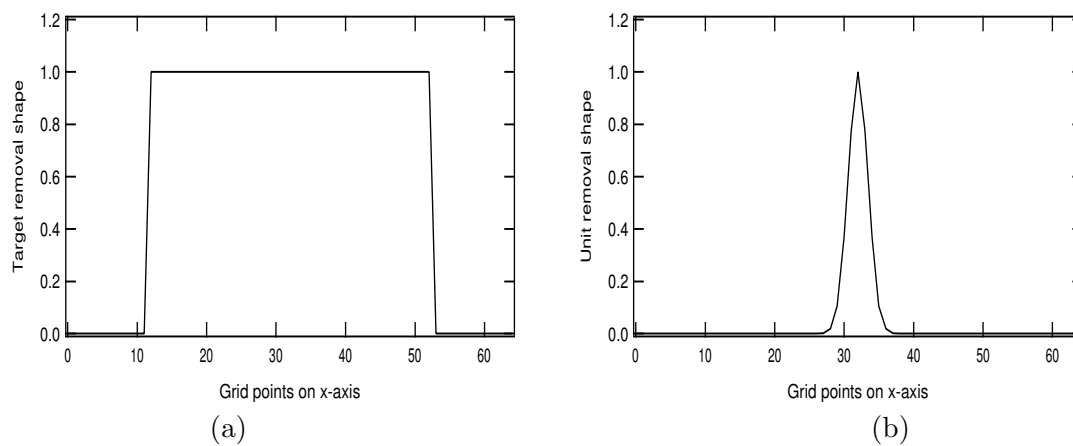


Figure 7: (a): The target removal shape on x -axis; and (b): the Gaussian unit removal shape on x -axis.

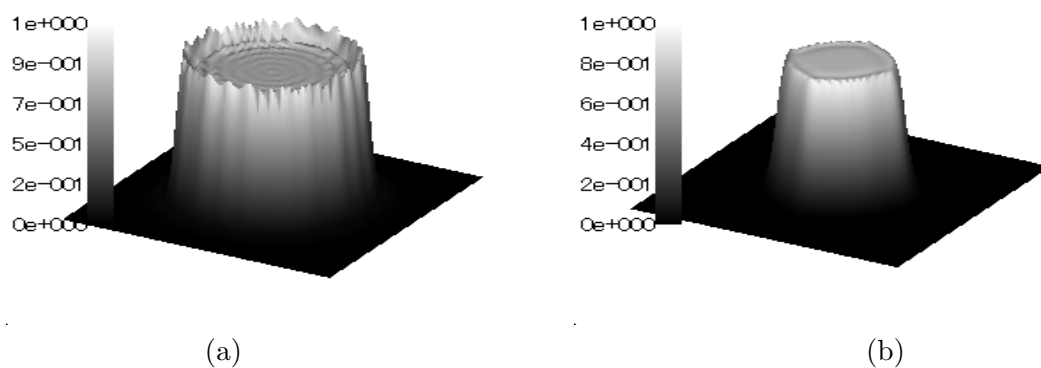


Figure 8: Removal shape produced by (a) Method A, (b) Method B.

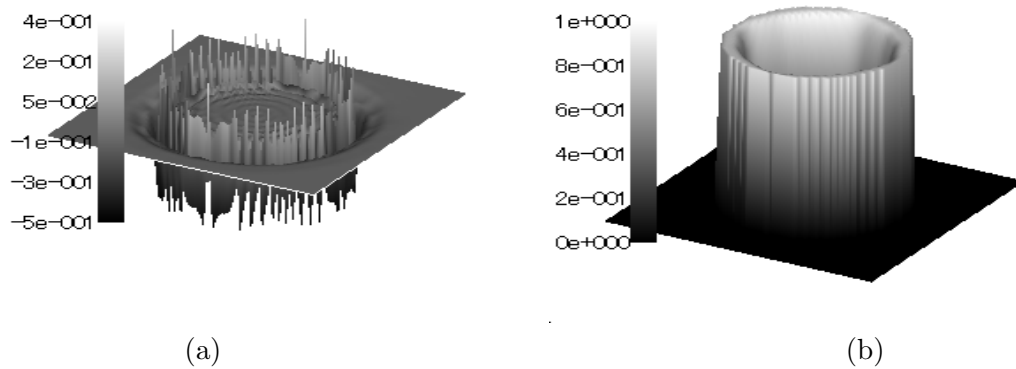


Figure 9: Residual error shape produced by (a) Method A, (b) Method B.

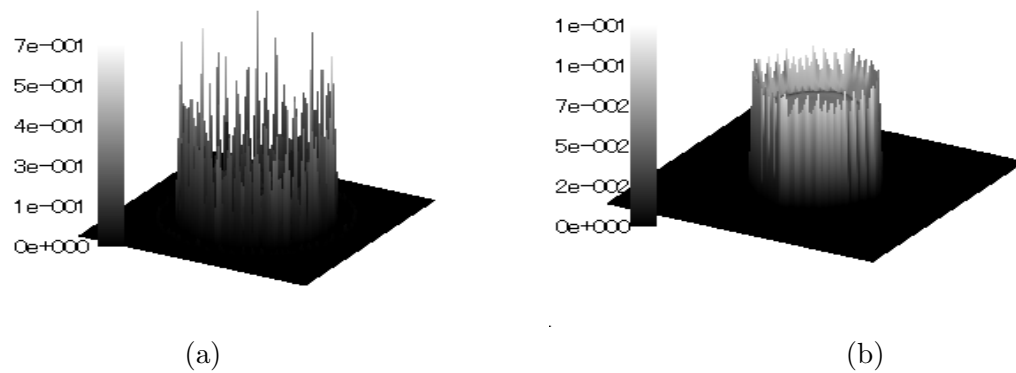


Figure 10: Dwell time distribution produced by (a) Method A, (b) Method B.

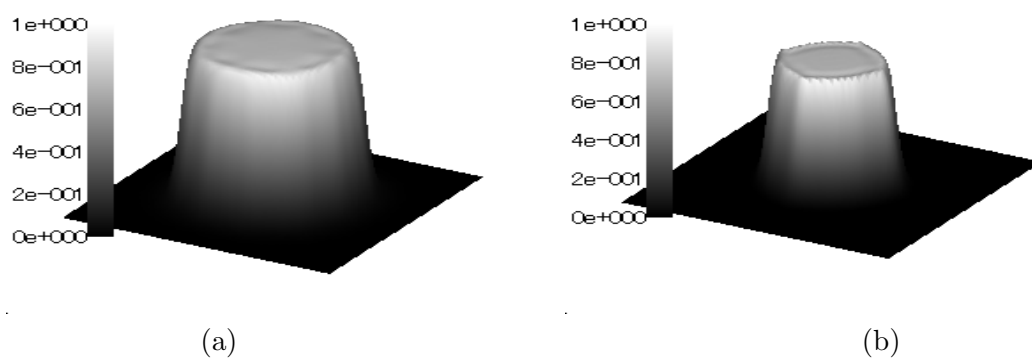


Figure 11: Removal shape produced by (a) Method A-B, (b) Method B-A.

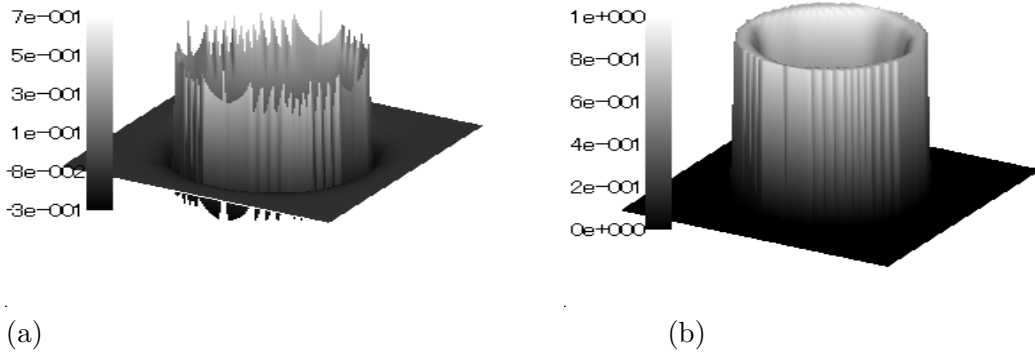


Figure 12: Residual error shape produced by (a) Method A-B, (b) Method B-A.

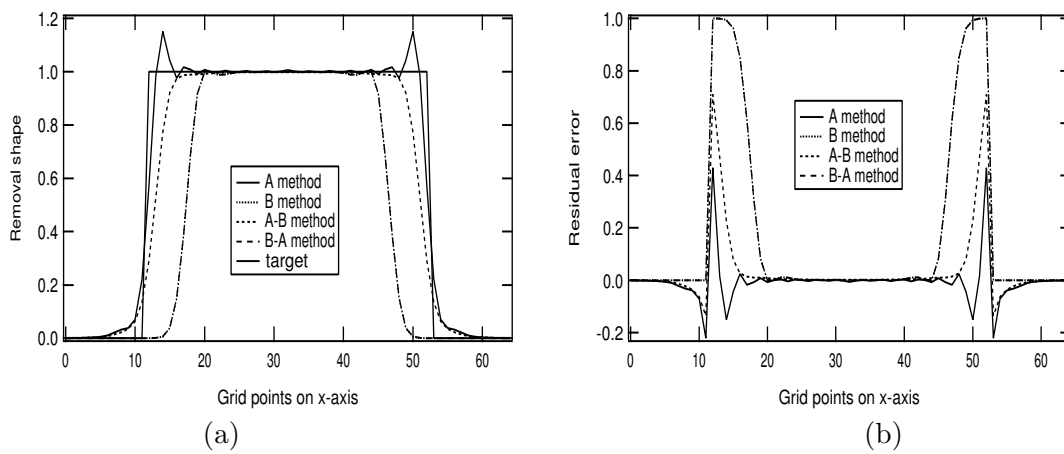


Figure 13: Comparisons of different methods for (a): the removal shape on x -axis; and (b): the residual error shape on x -axis.

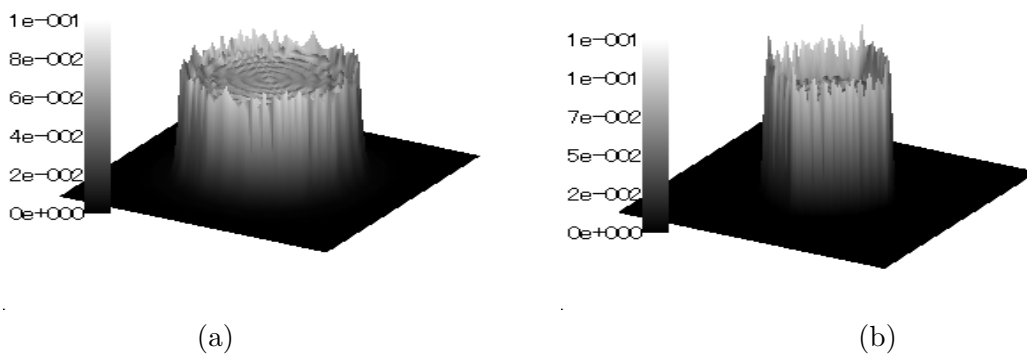
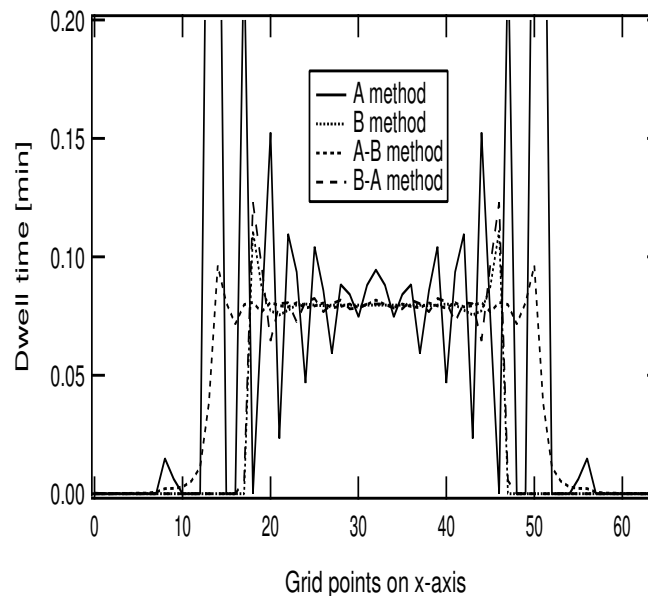


Figure 14: Dwell time distribution produced by (a) A-B Method, (b) B-A Method.

Figure 15: Dwell time distribution shape on x -axis.

numerical calculation, after calculating the dwell time distribution, are shown in Figs. 8 (a) and (b). The two-dimensional residual error shapes, i.e., the difference between the target removal shape, and the actual removal shape are shown in Figs. 9(a) and (b) for the two Methods A and B. From the PV and RMS of the residual error shape, it appears that in terms of process accuracy the FFT calculation technique is superior to the constraint problem method. On the other hand, in the constraint problem method the residual error only extends over a portion of the calculation domain. The dwell time distributions obtained finally are shown in Figs. 10(a) and (b) for the two Methods A and B.

The computational time and the required program size shown in Table 1 are considered as important factors in evaluating the calculation techniques. The CPU used for these calculations was an Intel Pentium 4 2.5GHz. It can be seen that Method A is about 4 times faster than Method B which is not only slow but also requires a memory that is 200 times larger than that required by A. Hence, it is concluded that the FFT calculation technique excels in speed as well as in memory.

Next, the dwell time is calculated using the combined techniques followed by an evaluation of the characteristics of these combined techniques. Here target removal shape, unit removal shape, and the number of data points used in the calculations are the same as for Methods A and B above.

The results for the removal shapes from the numerical calculation, after calculating the dwell time distribution, are shown in Figs. 11(a) and (b). Moreover, the two-dimensional residual errors are shown in Figs. 12(a) and (b). To compare the effectiveness of the two methods A and B and the two combined methods (A-B and B-A), the cross-section results

Table 1: Computational speed and program size.

	Method A	Method B	Method A-B	Method B-A
Computational speed	25.5s	94.3s	120.1s	120.1s
Program size	684kByte	136MByte	136MByte	136MByte

Table 2: Calculation result of PV, RMS, and average.

	Method A	Method B	Method A-B	Method B-A
PV	0.95163425	1	0.9993854307	1.00018126
RMS	0.112684814	0.38059697	0.141542047	0.41950714
Average	-0.04148624	0.20869080	0.021950515	0.28417357

for the removal shape and the residual error shape on the x -axis are shown in Fig. 13. The PV, RMS, and average of the calculation results are shown in Table 2 where the residual error can be evaluated quantitatively. Finally, the dwell time distributions obtained are shown in Fig. 14 and the cross-section drawing shown in Fig. 15. From these figures, some conclusions can be drawn which will be provided in the final section.

5 Conclusions

The following conclusions are arrived at from a comparison of the four techniques for calculating the dwell time distribution:

- 1) The FFT calculation technique (Method A) was the most accurate in terms of PV and RMS measures of the residual error shape. Hence, for calculations of the dwell time distribution, that requires overall processing accuracy, the FFT technique should be used.
- 2) It is preferable to use the constraint problem calculation technique (Method B) when excess removal occurs.
- 3) Excess removal does not occur when the removal shape is calculated by the FFT technique, which gives a highly accurate result with respect to the RMS and PV. Hence more favorable results can be obtained by calculating the removal shape by the constraint problem technique and calculating the target removal shape by the FFT technique (Method A-B). Therefore, it is concluded that Method A-B is the most effective here.
- 4) The removal shape, residual error, and dwell time distribution in the case of calculating only by the constraint problem technique almost coincides with the calculation result for calculating the removal shape by the constraint problem technique and calculating the target removal shape by the FFT technique (B-A Method).

References

- [1] M. Negishi, M. Ando, A. Deguchi, M. Takimoto, H. Narumi, N. Nakamura and H. Yamamoto, An on-machine coordinate measuring system for the canon super smooth polisher, Proc. SICE, 94 (1994), 941.
- [2] M. Ando, M. Negishi, M. Takimoto, A. Deguchi, N. Nakamura, M. Higomura and H. Yamamoto, Super-smooth surface polishing on aspherical optics, Proc. SPIE, 1720 (1992), 22.
- [3] R. Aspden, R. McDonough and F.R. Nitchie, Jr., Computer assisted optical surfacing, Appl. Opt., 11 (1972), 2739.
- [4] R.A. Jones, Optimization of computer controlled polishing, Appl. Opt., 16 (1977), 218.
- [5] K. Becker and K. Beckstette, M400 and P400 - A Pair of Machines for Computer-Controlled Fine Correction of Optical Surface, Ultraprecision in Manufacturing Engineering, Springer-Verlag, Berlin, (1988) 212.
- [6] A.P. Bogdanov, Optimizing the technological process of automated grinding and polishing of high-precision large optical elements with a small tod, Soviet J. Opt. Technol., 52 (1985), 409.
- [7] T. Matsumura and R. Ogasawara, Prediction of three-dimensional micro structures on FIB polishing, in: Proc. of The Japan Society of Precision Engineering, Spring meeting, B61, 2005, pp. 153-154, in Japanese.
- [8] M. Negishi, M. Ando, M. Takimoto, A. Deguchi and N. Nakamura, Studies on super-smooth polishing, T. Jpn. Soc. Precis. Eng., 62 (1996), 412, in Japanese.
- [9] J. Yang, K. Kobayashi, T. Sasaki and K. Nomura, Study on smooth polishing for optical element, in: Proc. of The Japan Society of Precision Engineering, Spring meeting, B22, 2004, pp. 133-134, in Japanese.